Modeling and Control of the Solar Hot Water System *

Tejaswinee Darure

September 2, 2021

Contents

*This research is carried out under Project IMPROVEMENT funded by European Commission with the European Regional Development Funds (ERDF) under the program *Interreg* SUDOESOE3/P3/E0901.

List of Figures

Abstract

Solar hot water system is becoming popular thanks to its environment friendly and economic advantages. In this work, the further improvement of economic operation through advanced control technologies is studied in detail. We consider a building infrastructure is equipped with hot water provided by solar thermal system. In this paper, economic model predictive control is exploited to estimate the demand and source management schedules considering the weather forecast errors.

1 Introduction

This work decibels the the advanced control method for the complete and complex system of the solar hot water. The system architecture in question is shown in Figure 1. Basically; solar radiation heats solar fluid and this heat flux is further used to heat the water in the hot water tank. With the intention of achieving utmost energy efficiency, thermal storage tank is integrated in the thermal circuit. This storage tanks provides the to water for the heating ventilation units that maintains the the temperature inside the buildings and ensures the comfort pf the occupants. In case of emergency and maintenance, an additional heat source i.e. heat pump is also integrated with the storage tank. In this work, the mathematical model of the entire system is presented.

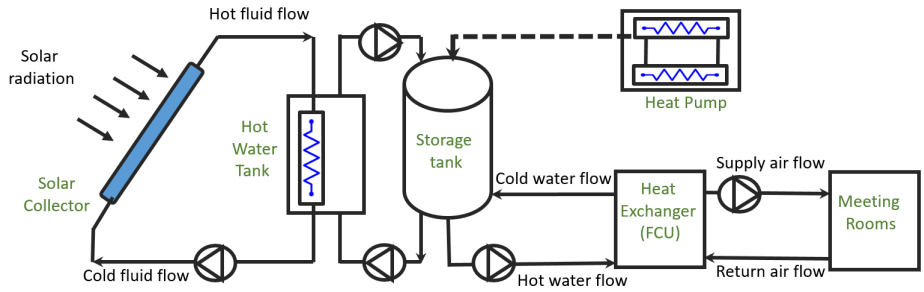

Figure 1: Solar Hot Water System

2 Mathematical Modeling of SHWS

The detailed mathematical models for all the units i.e. solar collector, hot water tank, storage tank, heat exchanger and heat pump etc.. are presented. For this exercise, the variables used are illustrated through the Figure 2.

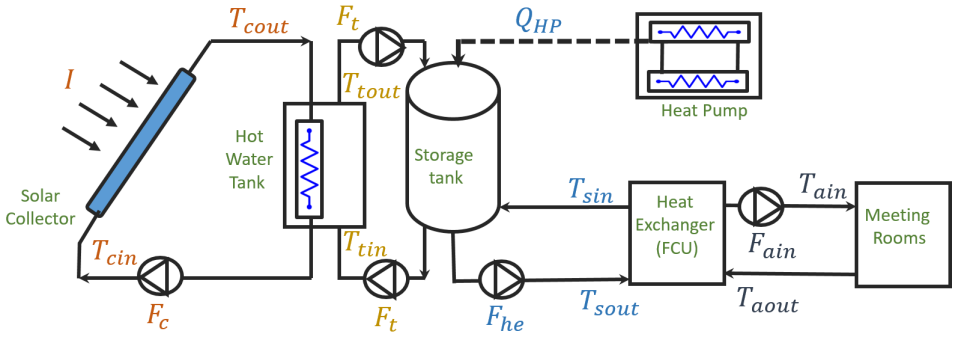

Figure 2: Variables - Solar Hot Water System

2.1 Solar Collector

The mass energy balance equation is the preferred approach in understanding the dynamics of the solar collector [1] [4]. The overall notion of mass energy balance equation is represented below:

$$\text{Accumulation of energy} = \text{Energy gain through solar radiation} + \text{Energy absorbed by the fluid} - \text{Energy loss}$$

The energy absorbed by the solar plate collector (Q_{solar}) is function of solar radiation and a straightforward relation can be given as,

$$Q_{solar} = A_c \eta I \tag{1}$$

where A_c is solar plate collector surface area (m^2) and η is optical efficiency (dimensionless) [1]. Heat flux Q_{fluid} gained by collector fluid can be formulated as following,

$$Q_{fluid} = \dot{m} c_c (T_{cout} - T_{cin}) \tag{2}$$

where $\dot{m}$ is the mass flow rate for the fluid (kg/s) and c_c is the specific heat of the fluid ($J/kg/K$). Moreover, heat loss in the solar collector can be given as below,

$$Q_{loss} = U_c A_c (T_{abs} - T_{oa}) \tag{3}$$

where U_c is the heat loss coefficient (W/m^2K) and T_{abs} is the absolute temperature of solar collector surface. Although, it is quite challenging to measure this temperature hence for simplicity the absolute temperature T_{abs} is replaced by the average of collector fluid temperature $T_{avg} = (T_{cin} + T_{cin})/2$. Now, the complete energy balance can be written using equations (1), (2) and (3),

$$Q_{acc} = Q_{solar} - Q_{fluid} + Q_{loss} \tag{4}$$

$$\rho_c c V_c \frac{dT_{out}}{dt} = A_c \eta I - \dot{m} c_c (T_{cout} - T_{cin}) + U_c A_c (T_{avg} - T_{oa}) \tag{5}$$

Note that mass flow rate $\dot{m}$ is expressed in terms of volumetric flow rate F_c as $\dot{m} = F_c \rho$. Hence after further rearranging the equation (5),

$$\frac{dT_{cout}}{dt} = \frac{A_c \eta}{\rho_c c_c V_c} I - \frac{F_c}{V_c}(T_{cout} - T_{cin}) + \frac{U_c A_c}{\rho_c c_c V_c}\left(\frac{T_{cin} + T_{cout}}{2} - T_{oa}\right) \tag{6}$$

For the control purpose, we represent the system into state space form for which state variable is T_{cout} ans controllable input is F_c while uncontrollable variables i.e. disturbances are I, T_{cin} and T_a.

$$\frac{dT_{cout}}{dt} = \frac{A_c \eta}{\rho_c c_c V_c} I + \frac{U_c A_c}{2\rho c V_c} T_{cin} + \frac{U_c A_c}{2\rho_c c_c V_c} T_{cout} - \frac{U_c A_c}{\rho c V_c} T_{oa} + \frac{1}{V_c} F_c T_{cin} - \frac{1}{V_c} F_c T_{cout} \tag{7}$$

2.2 Hot Water Tank : Heat Exchanger

In this section, the model of the hot water tank is discussed in detail. We consider the solar collector fluid heats the water in the hot water tank.

2.2.1 Co-current type Heat Exchanger

We assume the temperature in the tank is uniform and heat losses are negligible. The co-current model assumes that the inflows evolve in parallel in the same direction. The energy balance equation can be written as follows:

$$\frac{dT_{cin}}{dt} = \frac{F_c}{V_{ct}}(T_{cout} - T_{cin}) - \frac{U_t A_t}{\rho_c c_c V_{ct}}(T_{cin} - T_{tout}) \tag{8}$$

$$\frac{dT_{tout}}{dt} = \frac{F_t}{V_{ct}}(T_{tin} - T_{tout}) - \frac{U_t A_t}{\rho c V_{ct}}(T_{cin} - T_{tout}) \tag{9}$$

2.2.2 Counter-current type Heat Exchanger

The counterflow model assumes that the inflows evolve in parallel in the opposite direction and cross each other. The model is obtained from the one described in equation (8) and (9) considering the hypothesis that is described in the explanations, namely that the exchange temperatures must be crossed in the second part of the equations. We have T_{tout} which is replaced in the second part of the first equation by T_{tin} and we have T_cin which is replaced in the second part of the second equation by T_{cout}. We obtain the following model:

$$\frac{dT_{cout}}{dt} = \frac{F_c}{V_{ct}}(T_{cout} - T_{cin}) - \frac{U_t A_t}{\rho_c c_c V_{ct}}(T_{cin} - T_{tin}) \tag{10}$$

$$\frac{dT_{tout}}{dt} = \frac{F_t}{V_{ct}}(T_{tin} - T_{tout}) - \frac{U_t A_t}{\rho c V_{ct}}(T_{tout} - T_{cout}) \tag{11}$$

2.3 Thermal Heat Storage Tank

When solar energy is unavailable at nights and in cloudy weather, the continuous space heating is ensured using the Thermal Energy Storage (TES) tank. TES also allows to shift the peak hours energy consumption to off peak hours, significantly improving the system performance and saving energy costs. The pilot site in LNEG Lisbon is installed with a stratified TES that contains a dual heat exchanger. Hence, we present a detailed mathematical model of the stratified TES based on the energy balance equations.

The principle of stratified thermal storage tank is based on thermal stratification process where hot water sits on the cold water as depicted in Figure 3. In this work, we use the node based energy balance method, i.e. the energy balance equation for each node (12 in this case) are evaluated [**buckley2012development**]. Please note that the terms, node and layer are used interchangeably in the literature, hence for convenience we use the term layer. For the simplification of model, following assumptions are made [**rahman2015simplified**]:

1. The fluid used in the thermal storage tank is incompressible;
2. Pressure in the tank is assumed to be appropriate to avoid any fluid phase changes.
3. The mixing of layers due to buoyancy force has been considered negligible;
4. There is no mass flowing in or our of the storage tank, hence the mass balance equation is not considered.

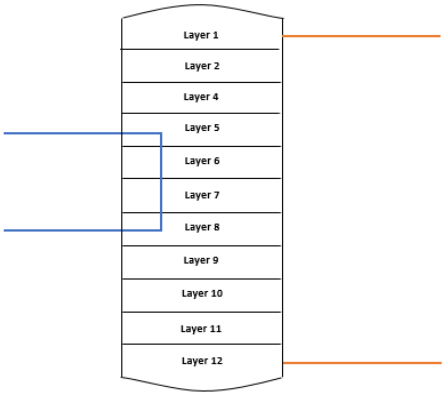

Figure 3: Stratified Thermal Storage Tank with 12 nodes

The energy balance equation will be different based on the position of the layer i.e. 1) boundary layers (layer 1, 12), 2) layers that are in direct contact with the heat transfer fluid of the solar collector (layer 5,6,7,8) or 3) the generic layer that only exchanges heat with the neighbouring layers (layer 2,3,4,9,10,11).

The temperature of generic layer is a function of the temperature of that layer itself and the temperatures of surrounding layers. The energy balance equation for i^{th} generic layer is given as follows (see Figure 3):

$$\frac{dT_{stl,i}}{dt} = \frac{\dot{V}_{stl}}{V_{stl}}(T_{stl,i+1} - T_{stl,i}) - \frac{U_{st}A_{stl}}{\rho_w c_w V_{stl}}(T_{stl,i} - T_{oa}) + \frac{k_{j,1}A_{stl}}{\rho_w c_w V_{stl}\Delta z}(T_{stl,i+1} - T_{stl,i}) + \frac{k_{j,2}A_{stl}}{\rho c V_{stl}\Delta x}(T_{stl,i-1} - T_{stl,i}) \quad (12)$$

where V_{stl} is the volume of the layer (m^3); $\dot{V}_{stl}$ is the volumetric flow rate (m^3/s); $T_{stl,i}$, $T_{stl,i-1}$ and $T_{stl,i+1}$ represent the temperature (^oC) of i^{th}, $i+1^{th}$ and $i-1^{th}$ layer; U_{st} is the heat transfer coefficient between the fluid in the storage tank and the atmospheric air considered constant (W/m^2K) and A_{stl} is the lateral area of the tank in contact with the layer (m^2); finally k_i is thermal conductivity of the water in the i^{th} layer (W/mK) and Δx is the height of the layer (m). It is clear from equation (17) that the thermal dynamics represent the energy gain due to the heat transfer fluid flow rate, energy transfer between lower and upper layers and finally the energy loss to the ambient.

Moreover, the layers in contact with the heat carrying fluid from solar collectors will have an additional term as shown in following equation representing

the heat gain due to the solar collector fluid flow rate.

$$\frac{dT_{stl,i}}{dt} = \frac{\dot{V}_{stl}}{V_{stl}}(T_{stl,i+1} - T_{stl,i}) - \frac{U_{st}A_{stl}}{\rho_w c_w V_{stl}}(T_{stl,i} - T_{oa}) + \frac{k_{j,1}A_{stl}}{\rho_w c_w V_t \Delta z}(T_{stl,i+1} - T_{stl,i}) \quad (13)$$

$$+\frac{U_{st,coil}A_{sc,coil}}{\rho_{sc}c_{sc}V_{st,coil}}(T_{stl,j} - T_{sc,out}) \quad (14)$$

Note that the term $\frac{U_{st,coil}A_{sc,coil}}{\rho_{sc}c_{sc}V_{st,coil}}(T_{stl,j} - T_{sc,out})$ represents the heat flux due to the solar collector fluid.

However, the boundary layers 1 and 12 have increased surface contact with the outside temperature, resulting in extra heat loss. The energy balance equations for these boundary layers are represented as follows:

$$\frac{dT_{stl,1}}{dt} = \frac{\dot{V}_{stl}}{V_{stl}}(T_{stl,2} - T_{stl,1}) - \frac{U_{st}A_{st,lateral}}{\rho c V_{stl}}(T_{stl,1} - T_{oa}) + \frac{k_{1,1}A_{stl}}{\rho c V_t \Delta z}(T_{stl,2} - T_{stl,1}) \quad (15)$$

$$\frac{dT_{stl,12}}{dt} = \frac{\dot{V}_{stl}}{V_{stl}}(T_{st,in} - T_{st,12}) - \frac{U_{st}A_{st,lateral}}{\rho c V_{stl}}(T_{stl,12} - T_{oa}) + \frac{k_{1,1}A_c}{\rho c V_t \Delta x}(T_{stl,11} - T_{stl,12}) \quad (16)$$

Note that $A_{st,lateral}$ represent the area of the lateral tank in contact with the layer plus area of the top section of the tank (m^2). Thus, the agglomeration of equations (17), (19) and (20) represents the dynamic behaviour of the stratified TES. It is worth to note that all the system parameters are used derived from the available pilot plant data.

The energy balance equation will be different based on the position of the layer i.e. 1) boundary layers (nodes 1, 12), 2) layers that are in direct contact with the heat transfer fluid of the solar collector (nodes 5,6,7,8) or 3) the generic layer that only exchanges heat with the neighbouring layers (nodes 2,3,4,9,10,11).

The temperature of generic layer is a function of the temperature of that layer itself and the temperatures of surrounding layers. The energy balance equation for i^{th} generic layer is given as follows (see Figure 3):

$$\frac{dT_i}{dt} = \frac{\dot{V}}{V_t}(T_{i+1} - T_i) - \frac{U_t A_t}{\rho c V_t}(T_i - T_a) + \frac{k_{j,1}A_t}{\rho c V_t \Delta z}(T_{i+1} - T_i) + \frac{k_{j,2}A_t}{\rho c V_t \Delta x}(T_{i-1} - T_i) \quad (17)$$

where V_t is the volume of the layer (m^3), $\dot{V}$ is the volumetric flow rate (m^3/s), T_i, T_{i-1} and T_{i+1} represent the temperature of i^{th}, $(i+1)^{th}$ and $(i-1)^{th}$ layer; U_t is the heat transfer coefficient between the fluid in the storage tank and the atmospheric air (considered constant in $W/(m^2 * K)$) and A_t is the lateral area of the tank in contact with the layer (in m^2); finally k_i is thermal conductivity of the water in the i^{th} layer (in $W/(m * K)$) and Δx is the height of the layer (in (m)). It is clear from equation (17) that the dynamics represent the energy

gain due to the heat transfer fluid flow rate, energy transfer between lower and upper layers and finally the energy loss to the ambient.

Moreover, the layers in contact with the heat carrying fluid from solar collectors will have an additional term as shown in following equation representing the heat gain due to the solar collector fluid flow rate.

$$\frac{dT_i}{dt} = \frac{\dot{V}}{V_t}(T_{i+1}-T_i) - \frac{U_t A_t}{\rho c V_t}(T_i - T_a) + \frac{k_{j,1} A_c}{\rho c V_t \Delta z}(T_{i+1}-T_i) + \frac{k_{j,2} A_c}{\rho c V_t \Delta x}(T_{i-1}-T_i) - \frac{U_s A_{coil}}{\rho c V_t}(T_j - T_{cout}) \tag{18}$$

Note that the term $\frac{U_s A_{coil}}{\rho c V_t}(T_j - T_{cout})$ represents the heat flux due to the solar collector fluid.

However, the boundary layers 1 and 2 have increased surface contact with the outside temperature, resulting in extra heat loss. The energy balance equations for these boundary layers are represented as follows:

$$\frac{dT_1}{dt} = \frac{\dot{V}}{V_t}(T_2 - T_1) - \frac{U_t A_{t,ts}}{\rho c V_t}(T_1 - T_a) + \frac{k_{1,1} A_c}{\rho c V_t \Delta z}(T_2 - T_i) \tag{19}$$

$$\frac{dT_{12}}{dt} = \frac{\dot{V}}{V_t}(T_{in} - T_{12}) - \frac{U_t A_{t,ts}}{\rho c V_t}(T_{12} - T_a) + \frac{k_{1,1} A_c}{\rho c V_t \Delta x}(T_{11} - T_{12}) \tag{20}$$

Note that $A_{t,ts}$ represent the area of the lateral tank in contact with the layer plus area of the top section of the tank (in (m^2)).

Thus, the agglomeration of equations 17, 19 and 20 represents the dynamic behavior of the TES.

2.4 FCU - heat exchanger

In general FCU unit comprises the fan and heat exchanger. The required air flow rate is set through the thermal zones controller. Hence, for this heat exchanger model, demand air flow rate can be considered as perturbation. Thus for this work, we consider the shell-tube type heat exchanger where the hot water in shell from the thermal storage tanks heat the supply air to required temperature. [3] explains the detailed model of the heat exchanger. Motivated from the mentioned reference, the mathematical formulation is customized for the water-air type shell-tube heat exchanger. Further following the same approach of energy balance, foll wing equations can be written for the shell side and tube side

$$\rho_a c_a V_{he} \frac{dT_{aout}}{dt} = \rho_a c_a F_a T_{ain} - \rho_a c_a F_a T_{aout} - \frac{k A_t}{\Delta z}(T_{aout} - T_{sin}) \tag{21}$$

$$\rho c V_{he} \frac{dT_{sin}}{dt} = \rho c F_{he} T_{sout} - \rho c F_{he} T_{sin} - \frac{k A_o}{\Delta z}(T_{sin} - T_{aout}) - h A'_o (T_s - T_{oa}) \tag{22}$$

Note A_t, A_o represent the ares of tube a tube side and shell side respectively where h and k are coefficient of convective heat transfer for air and conductive

heat transfer coefficient and finally Δz is the length of the tube. Simplifying the above equations,

$$\frac{dT_{aout}}{dt} = \frac{F_a}{V_{he}} T_{ain} - \frac{F_a}{V_{he}} T_{aout} - \frac{kA_o}{\Delta z \rho_a c_{pa} V_{he}} (T_{aout} - T_{sin}) \tag{23}$$

$$\frac{dT_{sin}}{dt} = \frac{F_{he}}{V_{he}} T_{sout} - \frac{F_{he}}{V_{he}} T_{sin} - \frac{kA_o}{\Delta z \rho c_p V_{he}} (T_{sin} - T_{aout}) - \frac{hA'_o}{\rho c V_{he}} (T_s - T_{oa}) \tag{24}$$

2.5 Thermal zone model

In this work, we consider the pilot building (shown in Figure 4) defined under the project IMPROVEMENT, situated in Lisbon Portugal.

Figure 4: Pilot Plant - LNEG Lisbon Portugal

The pilot area under the consideration is shown in figure 5 that contains multipurpose room ($83m^2$), meeting room ($22m^2$) and three individual offices ($11m^2$ each). It is essential to understand the thermal behavior of the general air conditioning system that uses the air circulation to maintain the thermal comfort of the occupants. This will allow us to derive the mathematical model for FCU type HVAC systems. Please note that the thermal comfort of occupants comprises various indicators as zone temperature, humidity and CO_2 concentration inside the thermal zones. However, in this work, we focus only on the zone temperature as a thermal comfort indicator. The air conditioning schematic of the typical thermal zone is shown in Figure 6.

The thermal behavior of the space heating is well explained based on the first law of thermodynamics. Let us consider n is the total number of zones in the building [2]. For each zone i, $(i = 1, ..., 5)$, we denote the temperature of the zone by T_i. The mass flow rate of the supply air entering in the i-th zone is represented by $\dot{m}_i$ and the supply air temperature by T_{si}. For the winter scenarios where the space heating is required, we write the energy balance

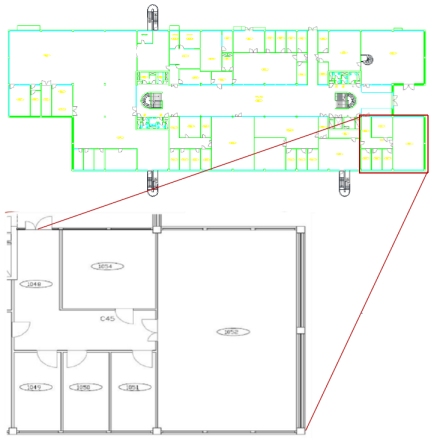

Figure 5: Pilot Schematic - LNEG Lisbon Portugal

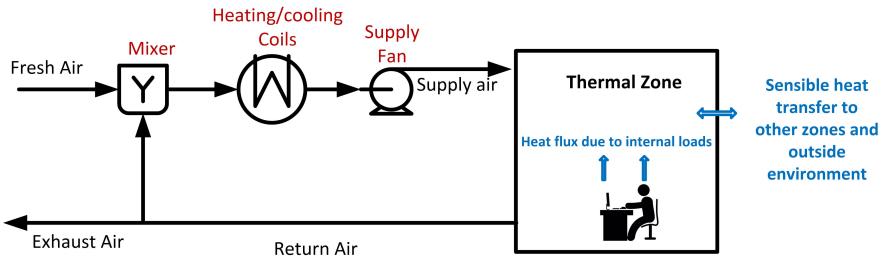

Figure 6: Schematic of air conditioning of a typical thermal zone

equation using first law of thermodynamics as the i-th zone:

$$\rho_a c_a V_i \frac{dT_i}{dt} = \dot{m}_i c_a \left(T_{si} - T_i\right) - \dot{Q}_{h,load_i} \tag{25}$$

with V_i the volume of zone i, ρ the air density and c_p the air specific heat coefficient. The rate of heat $\dot{Q}_{h,load_i}$ is the sensible heating load of zone i, that is, the net amount of energy that needs to be added to the zone to maintain a specified zone condition. Clearly, the sensible heating load is the sum of all heat losses and the internal heat gains. The heat loss for a zone i is due to the heat transfer from zone i to adjacent zones j and to the outside environment. Using thermal resistances, and denoting by q_i all internal heat gains due to the occupancy, electronic devices and solar gain to zone i, T_{oa} the outside air

temperature, the sensible heating load for zone i is

$$\dot{Q}_{h,load_i} = \frac{1}{R_{ext_i}}(T_i - T_{oa}) + \sum_{j=1,j\neq i}^{n} \frac{1}{R_{ij}}(T_i - T_j) - q_i \tag{26}$$

where $R_{ij} = R_{ji}$ is the thermal resistance between zone i and zone j, and R_{ext_i} is the thermal resistance between zone i and the exterior of the building. Now, substitute the heating load into equation (25), we get

$$C_i \frac{dT_i}{dt} = \dot{m}_i c_a (T_{si} - T_i) - \frac{1}{R_{ext_i}}(T_i - T_{oa}) - \sum_{j=1,j\neq i}^{n} \frac{1}{R_{ij}}(T_i - T_j) + q_i \tag{27}$$

where we set $C_i = \rho_a c_a V_i$ as the thermal capacitance of zone i.

It is obvious that to maintain the space heating requirements, the user should manipulate the heat gain through the supply air balancing the sensible heat loads. This implies that to control zone temperature T_i in the thermal comfort range, the user may manipulate the supply air temperature T_{si} or the supply air mass flow rate $\dot{m}_i$. This is a key that differentiates the thermal behavior of the HVAC systems based on VAV and FCU units respectively. Although in the case of LNEG pilot plant, the thermal zone temperature is maintained through the manipulation of the supply airflow while the supply air temperature is considered as constant.

The system of equations is implemented in the MATLAB simulink platform (Version 2017a) and tested against the test inputs. The example screenshot is shown in Figure 7.

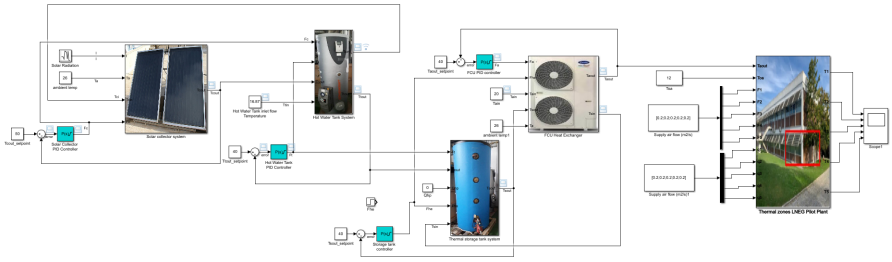

Figure 7: Screenshot- MATLAB SImulink implementation of the SHWS

2.6 State Space Model Representation

Please note that for simplicity the system is divided into two subsystems for obvious reasons. The solar collector, hot water tank and storage tank with heat exchanger unit can be considered as one subsystem while collective thermal zones are considered as another subsystem model. The supply air from the

thermal zones is not circulated hence the thermal network is distinct for these tow subsystems. Let us summarize all the equations here.

$$\frac{dT_{cout}}{dt} = \frac{A_c\eta}{\rho_c c_c V_c} I + \frac{U_c A_c}{2\rho c V_c} T_{cin} + \frac{U_c A_c}{2\rho_c c_c V_c} T_{cout} - \frac{U_c A_c}{\rho c V_c} T_{oa} + \frac{1}{V_c} F_c T_{cin} - \frac{1}{V_c} F_c T_{cout} \tag{28}$$

$$\frac{dT_{cin}}{dt} = \frac{F_c}{V_c}(T_{cout} - T_{cin}) - \frac{U_c A_c}{\rho_c c_c V_c}(T_{cin} - T_{tout}) \tag{29}$$

$$\frac{dT_{tout}}{dt} = \frac{F_t}{V_t}(T_{tin} - T_{tout}) - \frac{U_t A_t}{\rho c V_t}(T_{tout} - T_{cin}) \tag{30}$$

$$\frac{dT_{sout}}{dt} = \frac{F_t}{V_s} T_{tout} + \frac{Q_{HP}}{\rho c V_s} + \frac{F_{he}}{V_s}(T_{sout} - T_{sin}) \tag{31}$$

$$\frac{dT_{sin}}{dt} = \frac{F_{he}}{V_{he}} T_{sout} - \frac{F_{he}}{V_{he}} T_{sin} - \frac{kA_o}{\Delta z \rho c V_{he}}(T_{sin} - T_{aout}) - \frac{hA'_o}{\rho c V_{he}}(T_s - T_{oa}) \tag{32}$$

$$\frac{dT_{aout}}{dt} = \frac{F_a}{V_{he}} T_{ain} - \frac{F_a}{V_{he}} T_{aout} - \frac{kA_o}{\Delta z \rho_a c_a V_{he}}(T_{aout} - T_{sin}) \tag{33}$$

The matrices has to be checked again!

$$
\begin{bmatrix} \dot{T_{cout}} \\ \dot{T_{cin}} \\ \dot{T_{tout}} \\ \dot{T_{sout}} \\ \dot{T_{sin}} \\ \dot{T_{aout}} \end{bmatrix} = \begin{bmatrix} \frac{U_c A_c}{2\rho_c c_c V_c} & \frac{U_c A_c}{2\rho_c c_c V_c} & 0 & 0 & 0 & 0 \\ 0 & -\frac{U_c A_c}{\rho_c c_c V_c} & \frac{U_c A_c}{\rho_c c_c V_c} & 0 & 0 & 0 \\ 0 & 0 & -\frac{U_t A_t}{\rho c V_t} & \frac{U_t A_t}{\rho c V_t} & 0 & 0 \\ 0 & 0 & 0 & 0 & 0 & 0 \\ 0 & 0 & 0 & 0 & -\frac{kA_o}{\Delta z \rho c V_{he}} & \frac{kA_o}{\Delta z \rho c V_{he}} \\ 0 & 0 & 0 & 0 & \frac{kA_o}{\Delta z \rho_a c_a V_{he}} & -\frac{kA_o}{\Delta z \rho_a c_a V_{he}} \end{bmatrix} \begin{bmatrix} T_{cout} \\ T_{cin} \\ T_{tout} \\ T_{sout} \\ T_{sin} \\ T_{aout} \end{bmatrix}
$$

$$
+ \begin{bmatrix} 0 & 0 & \dots & & 0 \\ \vdots & \ddots & & & \vdots \\ \vdots & & \ddots & & \vdots \\ 0 & 0 & \dots & 0 & 0 \\ 0 & 0 & 0 & \frac{1}{\rho c V_s} & 0 \end{bmatrix} \begin{bmatrix} F_c \\ F_t \\ F_{he} \\ F_{ain} \\ Q_{hp} \end{bmatrix} + \begin{bmatrix} \frac{A_c \eta}{\rho_c c_c V_c} & -\frac{U_c A_c}{\rho c V_c} \\ 0 & 0 \\ 0 & 0 \\ 0 & 0 \\ 0 & -\frac{hA'_o}{\rho c V_{he}} \quad 0 \quad 0 \end{bmatrix} \begin{bmatrix} I \\ T_{oa} \end{bmatrix}
$$

$$
+ \begin{bmatrix} -\frac{1}{V_c} & \frac{1}{V_c} & 0 & 0 & 0 & 0 & 0 & 0 \\ \frac{1}{V_c} & -\frac{1}{V_c} & 0 & 0 & 0 & 0 & 0 & 0 \\ 0 & 0 & \frac{1}{V_t} & -\frac{1}{V_t} & 0 & 0 & 0 & 0 \\ 0 & 0 & \frac{1}{V_s} & 0 & \frac{1}{V_t} & -\frac{1}{V_t} & 0 & 0 \\ 0 & 0 & 0 & 0 & \frac{1}{V_t} & -\frac{1}{V_t} & 0 & 0 \\ 0 & 0 & 0 & 0 & 0 & 0 & -\frac{1}{V_{he}} & \frac{1}{V_{he}} \end{bmatrix} \begin{bmatrix} F_c T_{cout} \\ F_c T_{cin} \\ F_t T_{tout} \\ F_t T_{tin} \\ F_{he} T_{sout} \\ F_{he} T_{sin} \\ F_a T_{aout} \\ F_a T_{ain} \end{bmatrix} \tag{34}
$$

Observations:

- Depending on the values the eigenvalues of the matrix A may be positive and zero, resulting in an unstable system.
- Input matrix B is zero matrix which indicates inputs does not affect the behavior of states.
- Bilinear terms impose another challenge although it can be handled through feedback linearization techniques or nonlinear control methods.

3 Control System Design for SHWS

As shown in equation (2.6), the system dimension may cause the exponential copulation burden for optimization based control techniques. Hence, the distributed architecture cab be used in this case as shown in following Figure 8.

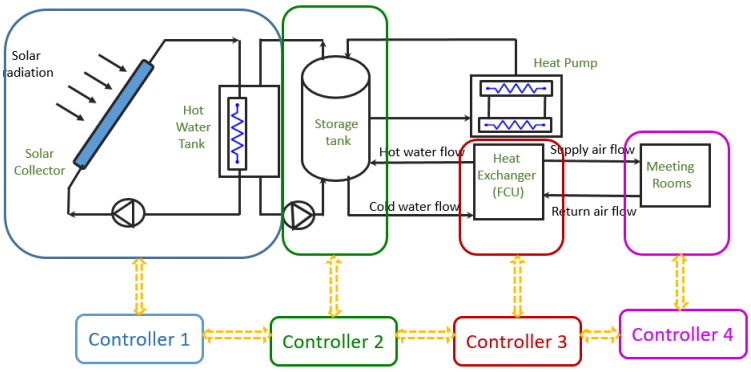

Figure 8: Distributed Architecture for Solar Thermal System

In the following subsections, all the controller from controller 1 to controller 4 are discussed in detail.

3.1 Controller 1: Solar Collector and Hot Water Tank

3.1.1 PID Controller

For control purpose, we pnly consider first two unit operations as shown in Figure 9. Further, Multiple PID controller configurations are possible. In this work, we consider two different schemes shown in figures.

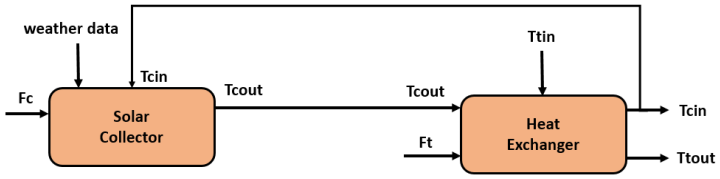

Figure 9: System Under Consideration

PID Controller Scheme I In this scheme, two independent PID controllers are implemented for solar collectors and hot water tank as shown in figure 10

and related matlab simulink screenshot is shown in 11. The results are shown in figure 12.

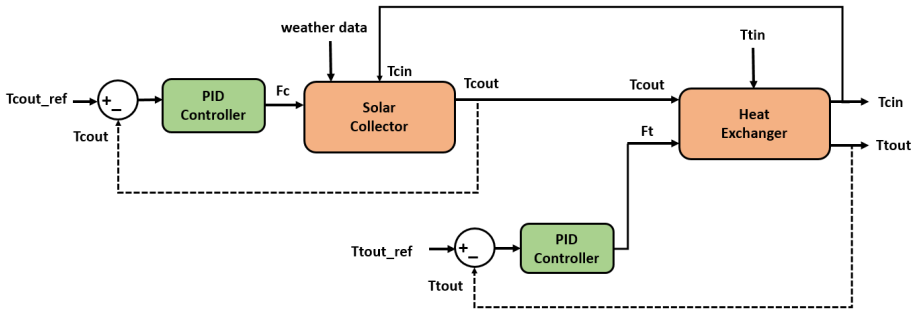

Figure 10: PID Controller Scheme I : Block Diagram

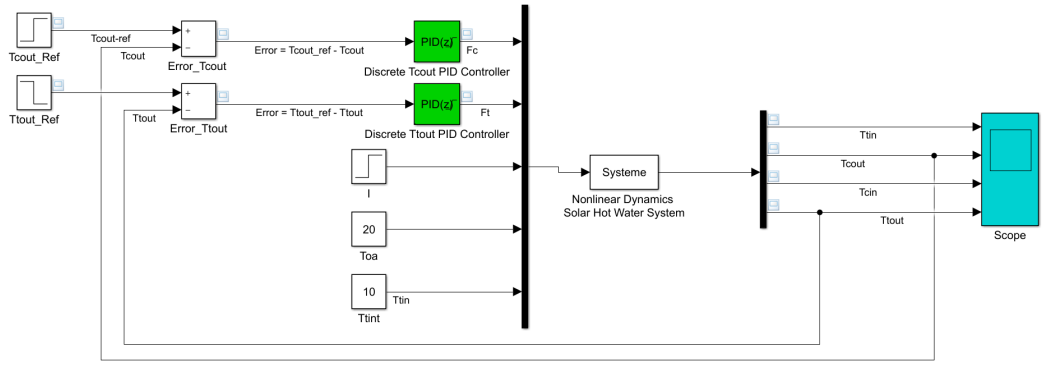

Figure 11: PID Controller Scheme I : Matlab Simulink

PID Controller Scheme II In this scheme, two independent PID controllers are implemented for solar collectors and hot water tank as shown in figure 13 and related matlab simulink screenshot is shown in 14. The results are shown in figure 15.

3.1.2 MPC Mathematical Framework

Considering only first two subsystems and related equations from equations (7); (10) and (24),

$$\frac{dT_{cout}}{dt} = \frac{A_c\eta}{\rho_c c_c V_c} I + \frac{U_c A_c}{2\rho c V_c} T_{cin} + \frac{U_c A_c}{2\rho_c c_c V_c} T_{cout} - \frac{U_c A_c}{\rho c V_c} T_{oa} + \frac{1}{V_c} F_c T_{cin} - \frac{1}{V_c} F_c T_{cout}$$

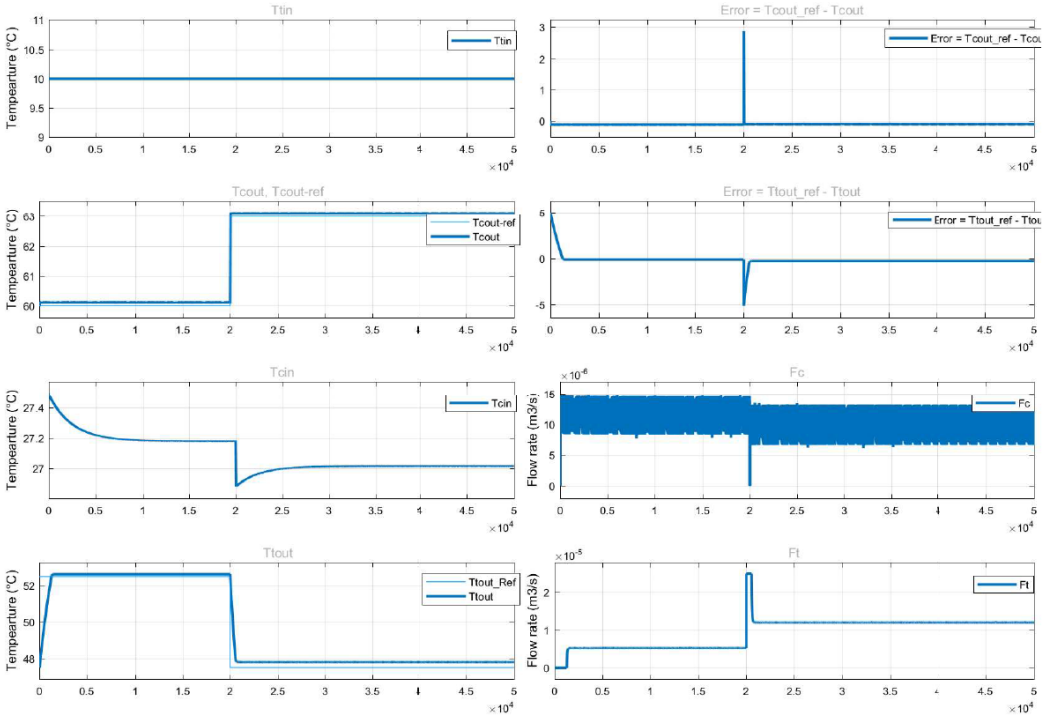

Figure 12: PID Controller Scheme I : Simulation Result

$$\frac{dT_{cin}}{dt} = \frac{F_c}{V_c}(T_{cout} - T_{cin}) - \frac{U_c A_c}{\rho_c c_c V_c}(T_{cin} - T_{tout}) \tag{35}$$

$$\frac{dT_{tout}}{dt} = \frac{F_t}{V_t}(T_{tin} - T_{tout}) - \frac{U_t A_t}{\rho c V_t}(T_{tout} - T_{cin}) \tag{36}$$

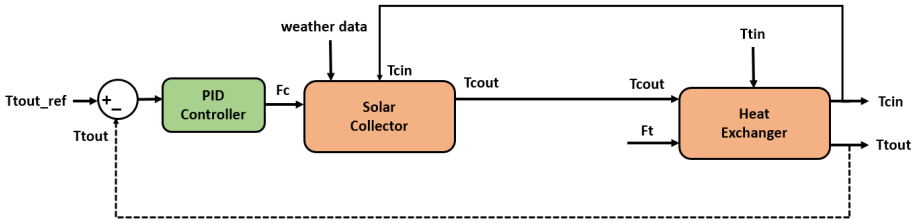

Figure 13: PID Controller Scheme II : Block Diagram

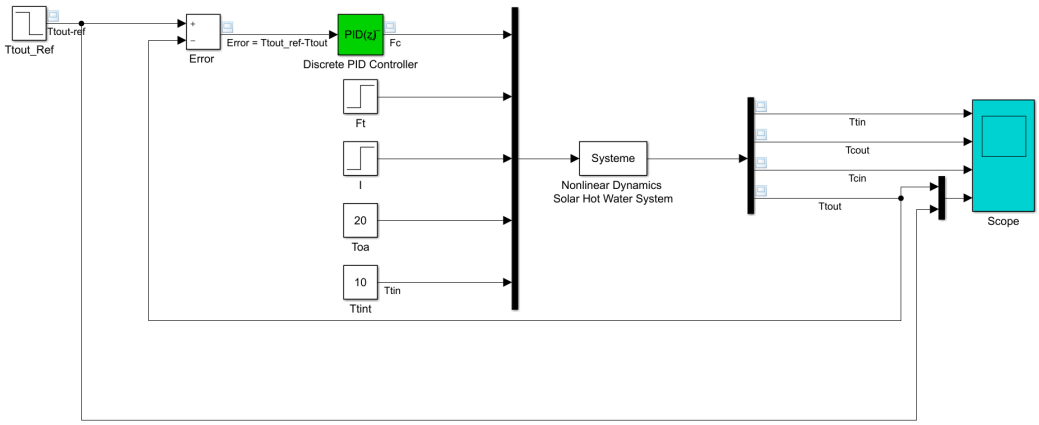

Figure 14: PID Controller Scheme II : Matlab Simulink

The subsystem state space can be written as follows:

$$\begin{bmatrix} \dot{T_{cout}} \\ \dot{T_{cin}} \\ \dot{T_{tout}} \end{bmatrix} = \begin{bmatrix} \frac{U_c A_c}{2\rho_c c_c V_c} & \frac{U_c A_c}{2\rho_c c_c V_c} & 0 \\ 0 & -\frac{U_c A_c}{\rho_c c_c V_c} & \frac{U_c A_c}{\rho_c c_c V_c} \\ 0 & 0 & -\frac{U_t A_t}{\rho c V_t} \end{bmatrix} + \begin{bmatrix} \frac{A_c \eta}{\rho_c c_c V_c} & -\frac{U_c A_c}{\rho c V_c} \\ 0 & 0 \\ 0 & 0 \end{bmatrix} \begin{bmatrix} I \\ T_{oa} \end{bmatrix}$$
$$+ \begin{bmatrix} -\frac{1}{V_c} & \frac{1}{V_c} & 0 & 0 & 0 \\ \frac{1}{V_c} & -\frac{1}{V_c} & 0 & 0 & 0 \\ 0 & 0 & \frac{1}{V_t} & -\frac{1}{V_t} & 0 \\ 0 & 0 & 0 & \frac{1}{V_t} & -\frac{1}{V_t} \end{bmatrix} \begin{bmatrix} F_c T_{cout} \\ F_c T_{cin} \\ F_t T_{tout} \\ F_t T_{tin} \end{bmatrix} \quad (37)$$

This state space can be linearized using jacobian matrix method and discretized for the sampling time of t=1s. There has been a great evolution in the

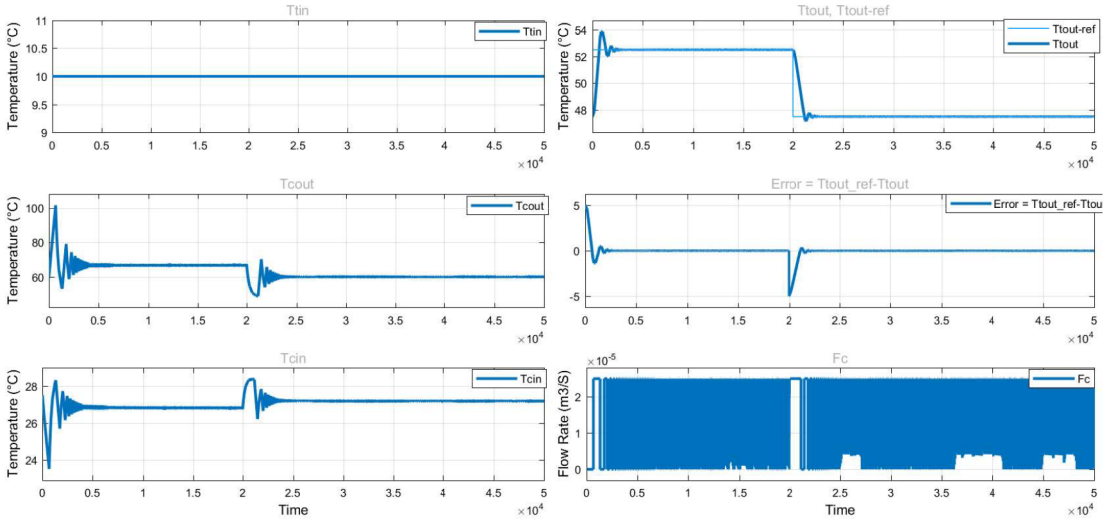

Figure 15: PID Controller Scheme II : Simulation Result

formulation of MPC in the literature. We consider the discrete-time state space model (3.1.2) which reads as:

$$\begin{aligned} x(k+1) &= Ax(k) + Bu(k) + Gd(k) \\ y(k) &= Cx(k) \end{aligned} \tag{38}$$

where $x(k) \in \mathcal{R}^{n_x}$ are the states representing the zone temperatures, $u(k) \in \mathcal{R}^{n_u}$ are the inputs of the system denoting the supply airflow, n_x and n_u are number of states and number of inputs respectively. $d(k) \in \mathcal{R}^{n_d}$ are the disturbances consisting the weather temperature and heat flux due to occupants and k is the discrete time. A, B and G are system dynamic matrices with appropriate dimensions.

Further, we present the optimization problem for the standard MPC as below,

$$\begin{aligned} &\underset{U_k}{\text{minimize}} \quad \mathcal{J}\left(U_k, x(k)\right) \\ &\text{subject to} \\ &x\left(k+j+1|\,k\right) = Ax\left(k+j|\,k\right) + Bu\left(k+j|k\right) \\ &\qquad\qquad +Gd\left(k+j|k\right) \qquad\qquad j = 0, \ldots, N-1 \\ &x^{min} \leq x\left(k+j|\,k\right) \leq x^{max} \qquad\qquad j = 0, \ldots, N-1 \\ &u^{min} \leq u\left(k+j|k\right) \leq u^{max} \qquad\qquad j = 0, \ldots, N-1 \\ &x\left(k|\,k\right) = x(k) \end{aligned} \tag{39}$$

where $\mathcal{J}$ is the functional representing the overall cost function, N is the prediction horizon, $U_k = \{u(k|k), \ldots, u(k+N-1|k)\}$ is the sequence of predicted

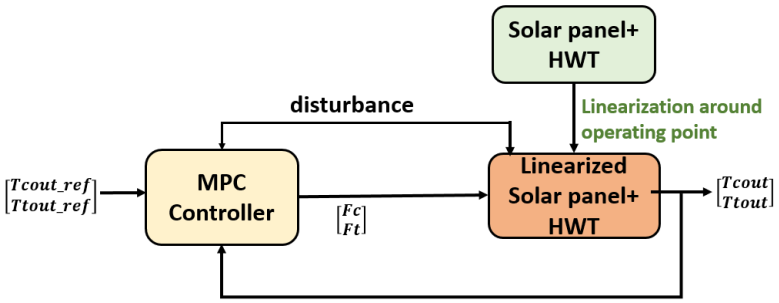

Figure 16: MPC Controller Scheme : Block Diagram

control inputs at time k. The bounds u^{min}, u^{max} on the input vector u, i.e. on the supply airflow rate represent the damper limits in the VAV box. The bounds on states x^{min}, x^{max} represent the soft bounds on the zone temperature to maintain a thermal comfort. Problem (41) is solved repetitively at each time k using the receding horizon principle for the current measured state $x(k)$ along with the predicted state variables $\{x\,(k+j|\,k)\}_{j=1}^{N}$. Assume that the forecast for the disturbances $\{d(k|k), \ldots, d(k+N-1|k)\}$ is available a prior. then the corresponding optimal sequence $U_k^{\star} = \{u^{\star}\,(k)\,, ...,\, u^{\star}\,(k+N-1)\}$ is obtained and the first element $u^{\star}\,(k)$ of this sequence is applied to the system. The procedure is repeated at time $k+1$, based on the new measured state $x\,(k+1)$.

Refer Houda's work for YALMIP MPC implementation and FDD, FTC analysis.

3.1.3 NMPC Mathematical Framework

Instead of linearizing the system at operating point, controller by defaukt considers the nonlinearity in the system. There are multiple ways to code the NMPC.

the dynamics of the considered solar hot water system is given as,

$$\frac{dT_{sc,out}}{dt} = \frac{A_{sc}\eta}{\rho_{sc}c_{sc}V_{sc}}I - \frac{F_{sc}}{V_{sc}}(T_{sc,out} - T_{sc,in}) + \frac{U_{sc}A_{sc}}{\rho_{sc}c_{sc}V_{sc}}\left(\frac{T_{sc,in}+T_{sc,out}}{2} - T_{oa}\right)$$

$$\frac{dT_{sc,in}}{dt} = \frac{F_{sc}}{V_{ct}}(T_{sc,out} - T_{sc,in}) - \frac{U_{ht}A_{ht}}{\rho_{sc}c_{sc}V_{ct}}(T_{sc,in} - T_{ht,out})$$

$$\frac{dT_{he,out}}{dt} = \frac{F_{he}}{V_{ce}}(T_{he,in} - T_{he,out}) - \frac{U_{he}A_{he}}{\rho_{w}c_{w}V_{ce}}(T_{sc,in} - T_{he,out})$$

For uniformity and simplicity of the nomenclature, the states of the system are $x = [T_{sc,out}, T_{sc,in}, T_{he,out}]$, the inputs $u = [F_{sc}, F_{he}]$ where disturbances $d =$

$[I, T_{oa}, T_{he,in}]$. Hence, the nonlinear system dynamics can be represented as below:

$$x(k+1) \quad = \quad f(x(k), u(k), d(k)) \tag{40}$$

where f represents the equations 40, 40 and 40. It is worth to note than these set of differential equations are solved for the time span of 60 minutes, coherent to the disturbance data sampling. Further, we present the optimization problem for the standard NMPC as below,

$$\begin{aligned}
&\underset{U_k}{\text{minimize}} \qquad \mathcal{J}\left(U_k, x(k)\right) \\
&\text{subject to} \\
&x\left(k+j+1 \middle| k\right) = f(x\left(k+j \middle| k\right), u\left(k+j|k\right), d\left(k+j|k\right) \\
&\qquad\qquad\qquad\qquad\qquad\qquad\qquad\qquad\qquad\qquad j = 0, \ldots, N-1 \\
&x^{min} \leq x\left(k+j \middle| k\right) \leq x^{max} \qquad\qquad j = 0, \ldots, N-1 \\
&u^{min} \leq u\left(k+j|k\right) \leq u^{max} \qquad\qquad j = 0, \ldots, N-1 \\
&x\left(k \middle| k\right) = x(k)
\end{aligned}$$

where $\mathcal{J}$ is the functional representing the overall cost function, N is the prediction horizon, $U_k = \{u(k|k), \ldots, u(k+N-1|k)\}$ is the sequence of predicted control inputs at time k. The bounds u^{min}, u^{max} on the input vector u, i.e. on the solar heat fluid flow rate and water flow rate that represent the fluid pump limits. The bounds on states x^{min}, x^{max} represent the soft bounds on the temperatures to compel the values to remain the predefined range. Optimization problem is solved repetitively at each time k using the receding horizon principle for the current measured state $x(k)$ along with the predicted state variables $\{x\left(k+j \middle| k\right)\}_{j=1}^{N}$. Assume that the forecast for the disturbances $\{d(k|k), \ldots, d(k+N-1|k)\}$ is available a prior. then the corresponding optimal sequence $U_k^{\star} = \{u^{\star}\left(k\right), ..., u^{\star}\left(k+N-1\right)\}$ is obtained and the first element $u^{\star}\left(k\right)$ of this sequence is applied to the system. The procedure is repeated at time $k+1$, based on the new measured state $x\left(k+1\right)$.

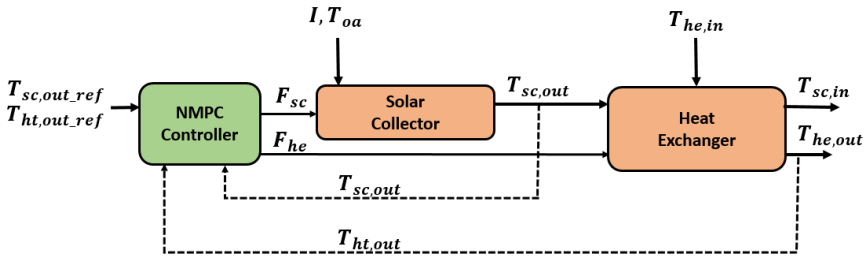

Figure 17: NMPC Control Scheme

The attempted ways:

1. Without any external packages

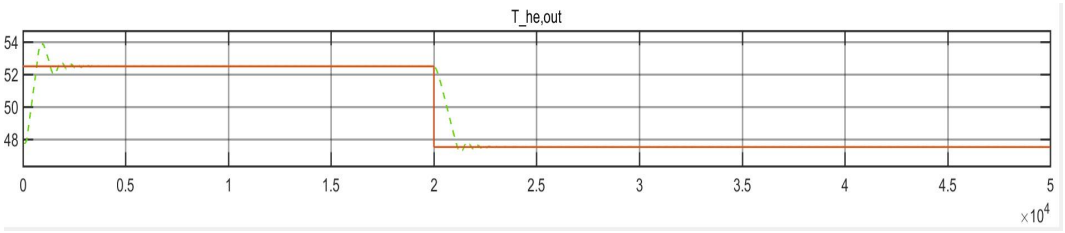

Figure 18: NMPC Control Scheme

2. Using YALMIP package

4 Project Update

All deliverable and related drafts are available on Improvement Project Cloud

4.1 Past work

1. **System information and communication with LNEG**
   - All the meeting information and received information about pilot plant can be found on github or shared drive.
   - Installed (purchased) controllers and schemes are important information for next task in WP4 to fulfill demonstration task.
   - Information contact: Instrumentation, scada and data; **Joao Corea;** Process flow: **David Loureiro**, Delierables contact: **Jorge Facao**, manager: **Ana Estanqueiro**
2. **Mathematical modeling**
   - First principle based models for each unit for LNEG pilot plant
   - Refer Github to access all code and simulink files (IST models are also available)
   - Prepared journal paper draft on github
   - System characteristics used from Pilot plant
3. **Controller design adn testing**
   - Various PID configurations have been simulated: Two PIDS, Single PID ! Refer notes for more info.
   - Single PID config is tuned with LNEG pilot plant installtion
   - MPC controller have been implemented in matlab using YALMIP (code on githib)

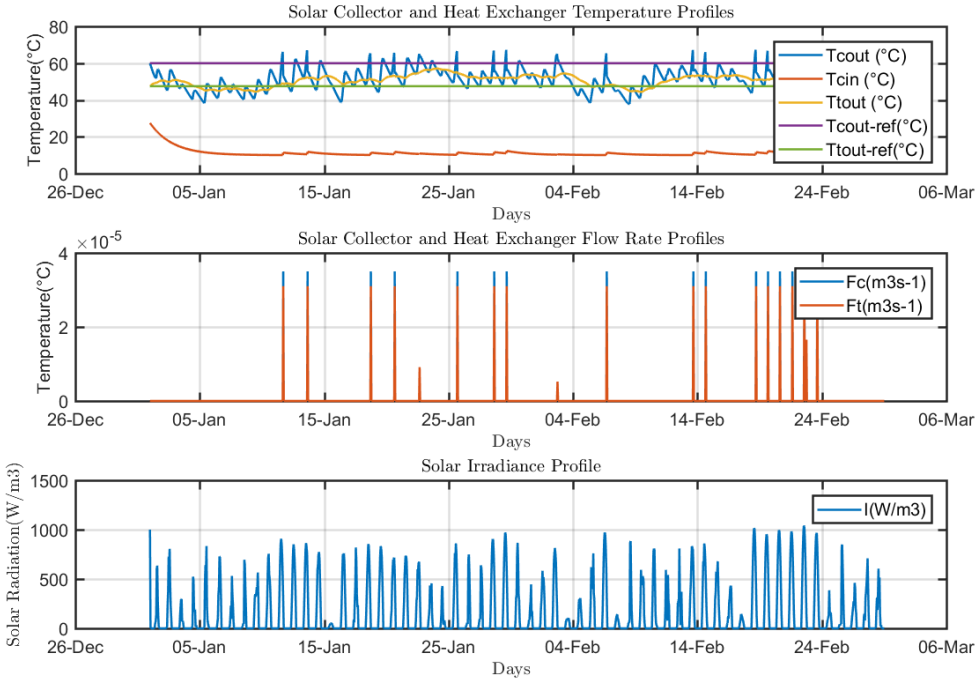

Figure 19: NMPC Controller : Simulation Result

- Fault diagnosis and tolerant conotrolled impleme,ted by Houda
- NMPC is implemented using Tomlab and code on github (for information refer

4. **Project milestones**

   - Paper contribution with the project team describing MPC literature review for microgrids (available online)
   - **Deliverables:**
     1. **D4.2.1** Control algo: completed and final draft submitted to coordinator
     2. **D3.1.1** Contribution provided to LNEG 3. **D3.2.1** Pilot info: completed from our side and LNEG follow up required
   - Three consortium meetings and presentations
   - Two publications in pipeline

4.2 Future Plan

Note, it was my personal plan which was an effort to align project requirements and personal interest. This can be changed according to the expertise of new contributor.*

Delievarble	EL	Deadline	Coordinator	Participants
D1.4.1. Current Regulatory Framework and Proposal		30/09/2022	JA	CNH2,AAE,UPVD,IST,UCO
D1.4.2. Technical and Market Codes Review		30/09/2022	JA	CNH2,AAE,UPVD,IST,UCO
D1.5.1. Implantation Plans		30/12/2022	CNH2	AAE,UPVD,IST,UCO
D3.1.1. Technology Prospective Analysis for Thermal Energy Storage System for cooling and heating applications		31/01/2021	IST	LNEG,UPDV
D3.2.1. Report on Technical Specification of the IMPROVEMENT heating and cooling system		30/06/2021	UPVD	IST,LNEG,CNH2
D4.2.1. Report on advanced renewable-energy-based heating and cooling system		30/06/2021	IST	LNEG,UPVD,CNH2
D4.2.1 Report on Advanced Energy Management System for Renewable Energy based Microgrid with combined generation of cool, heat and electrical power and multiple Energy Storage Systems		31/03/2021	UPDV	CNH2,IST,ENSMA
D4.5.1. Test bed deployment to validate the IMPROVEMENT's energy management system		30/06/2022	UPDV	CNH2,IST,ENSMA,LNEG,AAE
D4.5.2. Factory Acceptance Test to validate the IMPROVEMENT's energy management system		30/06/2022	UPDV	CNH2,IST,ENSMA,LNEG,AAE

Figure 20: Deliverable Commitment

- **Modeling and control design for Thermal storage tank**
  1. Model is available, can be fine tuned for control purpose
  2. NMPC controller code can be recycled
  3. Conference paper can be published
- **Complete system integration**
  1. Instead of considering standalone models and controller distributed architecture can be proposed
  2. Performance can be compared with centralized MPC
  3. Models are available as well as the appropriate code: fine tuning will be needed.
- **Weather forecast**

  Note: These plans were purely for publication purpose.
- **Project plans**
  1. **D3.2.1** needs follow up and final submission. LNEG will have to add their parts. Deadline was June 30th.
  2. **D4.5.1 and D4.5.2** are due in June 2022 which requires the plan of controller hardware implementation and demonstration details. Suggestion: Installed controlled can be used wisely to fulfill this requirement (e.g.cascade control, interlocks and safety etc..)
  3. **Consortium meeting**
     Date: November 21st
     Presentation: coordination with IST, LNEG and CNH2 for WP4 progress update and prepare slides, slots for everyone
- **Demonstration ideas**

- Using exiting controller to improve performance e.g. **deltaPlus** solar collector controller can be used in cascade config, extra interlocks and safety can be added, time scheduling is possible
- **Schieder SCADA**: it can access weather data, that be used for control purpose, in-built MPC function may available, Gain scheduling PIDs can be implemented.
- **Data based methods**: Based opn collected data, explicit gain/control strategy can be designed that can save energy as well as cost.

References

[1] J Buzás et al. "Modelling and Simulation of a Solar Thermal System". In: *IFAC Proceedings Volumes* 30.5 (1997), pp. 143–147.

[2] Tejaswinee Darure. "Contribution to energy optimization for large-scale buildings: an Integrated approach of diagnosis and economic control with moving horizon". PhD thesis. Université de Lorraine, 2017.

[3] James B Riggs and Mohammed Nazmul Karim. *Chemical and Bio-process Control: James B. Riggs, M. Nazmul Karim*. Prentice Hall, 2006.

[4] I Zeghib and A Chaker. "Simulation of a solar domestic water heating system". In: *Energy Procedia* 6 (2011), pp. 292–301.